Int J. Solids Structures, 1977, Vol. 13, pp. 445–455. Pergamon Press. Printed in Great Britain

INFLUENCE OF BOUNDARY CONDITIONS ON THE STABILITY OF A COLUMN UNDER NON-CONSERVATIVE LOAD

PAULI PEDERSEN
Department of Solid Mechanics, The Technical University of Denmark, Lyngby, Denmark

(*Received* 24 *June* 1976)

Abstract—The cantilever follower force problem with external damping is extended to a three-parameter case, including a concentrated mass, a linear elastic spring, and a partial follower force at the free end. As a result of the study an unexpected, hitherto unrecognized feature of stability/vibration is identified.

Normally, the boundary conditions have great influence on the stability limits. However, it is proved that there exists a force at which the critical frequency is independent of all three boundary parameters. The characteristics of this force/frequency combination are discussed in detail, especially in relation to the corresponding eigenfunctions.

Also a direct study of the onset of flutter as a function of the boundary parameters is included.

INTRODUCTION

During the past two decades the non-conservative (circulatory as classified by Ziegler[1]) stability problem of a cantilever subjected to a follower force has been the subject of a number of papers, see Bolotin[2], Herrmann[3] and Leipholz[4]. A study including an end mass is presented by Pflüger[5], and the problem with partial follower force has been studied by Petterson[6], König[7], Kordas and Zyczkowski[8], and Herrmann and Bungay[9]. The effect of damping has been studied by Leipholz[10], Nemat-Nasser, Prasad and Herrmann[11], Bolotin and Zhinzher[12], and by Plaut and Infante[13]. The present paper treats the continuous cantilever, follower force, externally damped problem with the boundary conditions, given by three parameters at the free end, corresponding to a concentrated mass, a linear elastic support and a partial follower force. A thorough consideration of how response depends on the boundary parameters leads to some additional insight about the follower force problem.

As a result of the study, a higherto unrecognized feature of stability/vibration is identified. This feature is the existence of a characteristic point of the characteristic curves of instability in the force/frequency coordinate system, i.e. it is proved that there exists a value of force for which the natural frequency is independent of the concentrated mass, the support stiffness and the follower angle of the force. Stated in other terms, all characteristic curves corresponding to first and second natural frequencies intersect at a *common* force/frequency point λ_C, ω_C. The existence of such points for higher order pairs of eigenfrequencies is also evident.

To understand this feature from a physical point of view it is necessary to study the corresponding eigenmodes. At λ_C, ω_C the eigenmode can be represented as a linear combination of two well-defined functions. The specific combination is first determined by the path, i.e. by the value of $d\omega/d\lambda$ associated with a particular curve. Thus at the common point λ_C, ω_C the eigenmode reflects the value of the boundary parameters.

Solutions in terms of eigenfrequencies and degree of instability as a function of load, together with initial flutter load as a function of external damping are given for various boundary parameters. Then the study is concentrated directly on prediction of the onset of flutter and divergence as a function of the boundary parameters, treating these as continuous variables.

1. INSTABILITY ANALYSIS—FLUTTER AND DIVERGENCE

As shown in Fig. 1, we consider a uniform continuous cantilever of length L, bending stiffness EI, and mass per unit length ρA. At the free end the boundary conditions are given by three parameters, corresponding to a concentrated mass M, a linear elastic support of stiffness K, and a force P which follows according to the parameter η. Viscous external damping per unit mass B is included.

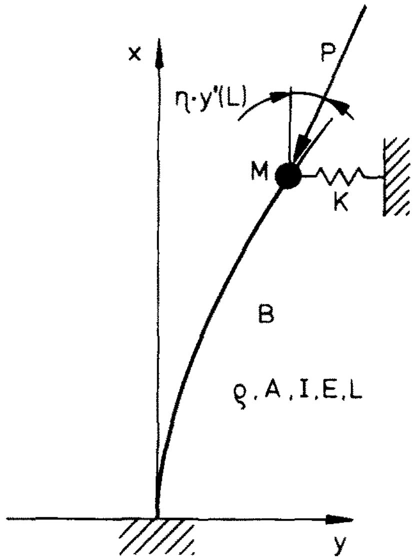

Fig. 1. Extended follower force problem.

Non-dimensional space ξ and time τ are defined by

$$\xi = X/L, \quad \tau = t/\sqrt{(\rho A L^4/(EI))}. \tag{1.1}$$

The differential equation of motion is

$$\bar{y}''''(\xi, \tau) + \lambda \bar{y}''(\xi, \tau) + \ddot{\bar{y}}(\xi, \tau) + \beta \dot{\bar{y}}(\xi, \tau) \equiv 0 \tag{1.2}$$

with the non-dimensional force and damping coefficients defined by

$$\lambda = PL^2/(EI), \quad \beta = BL^2\sqrt{(\rho A/(EI))}. \tag{1.3}$$

By separation of variables

$$\bar{y}(\xi, \tau) = y(\xi)\psi(\tau), \tag{1.4}$$

the time-dependent part of the solution is governed by the equation

$$\ddot{\psi}(\tau) + \beta\dot{\psi}(\tau) + \phi^2\psi(\tau) = 0, \quad \phi^2 = \zeta \pm i\epsilon. \tag{1.5}$$

As shown in the next section the complex constant ϕ^2 is the eigenvalue of the eigenvalue problem governed by the separated differential equation of space together with the actual boundary conditions.

In this section we shall, for the completeness of presentation, answer the question of stability corresponding to a given ϕ^2. A solution to eqn (1.5) in the form

$$\psi(\tau) = e^{(\alpha \pm i\omega)\tau} \tag{1.6}$$

implies stability for $\alpha \leq 0$, and instability for $\alpha > 0$ with static instability (divergence) for $\omega = 0$ and dynamic instability (flutter) for $\omega \neq 0$. Inserting (1.6) in eqn (1.5), we obtain

$$\alpha \pm i\omega = \frac{-\beta}{2}\left\{1 \pm \frac{1}{\beta}\sqrt{[(\beta^2 - 4\zeta) \mp i4\epsilon]}\right\}. \tag{1.7}$$

Thus *instability for* $\beta < 0$ follows directly. In the following we therefore assume $\beta > 0$.

Now defining c, d by

$$c \pm id = \sqrt{[(\beta^2 - 4\zeta) \mp i4\epsilon]}, \tag{1.8}$$

the physical quantities α, ω are given by

$$\alpha = -\frac{\beta}{2}\left(1 \pm \frac{c}{\beta}\right), \quad \omega^2 = \frac{d^2}{4} = \frac{\epsilon^2}{c^2}, \tag{1.9}$$

and we see that the criterion for instability is

$$c^2 > \beta^2. \tag{1.10}$$

Then eqn (1.8) is solved for c^2 giving

$$c^2 = \frac{1}{2}(\beta^2 - 4\zeta) + \sqrt{\left(\frac{1}{4}(\beta^2 - 4\zeta)^2 + 4\epsilon^2\right)}, \tag{1.11}$$

from which it follows that we have *instability for* $\zeta < 0$. What then remains to determine is the domain of instability for $\beta > 0$, $\zeta > 0$.

We see from eqn (1.11) that c^2 increases monotonically with ϵ^2, and thus $\epsilon^2 > \epsilon_C^2$ causes instability. The cricital value ϵ_C^2 is determined by $c^2 - \beta^2 = 0$, and we thus have *instability for*

$$\epsilon^2/\zeta > \beta^2, \tag{1.12}$$

as stated in [10].

Summing up, we conclude that the cases of (a) negative damping, $\beta < 0$, (b) a negative real part of the constant ϕ^2, $\zeta < 0$, and (c) a dominating imaginary part of the constant ϕ^2, $(\epsilon^2/\zeta > \beta^2)$ all correspond to instability.

Only with a zero imaginary part of the constant ϕ^2, is the instability of static type. Onset of flutter corresponding to point (c) above occur at the frequency

$$\omega_F^2 = \epsilon^2/\beta^2, \tag{1.13}$$

as seen from eqn (1.9) with $c^2 = \beta^2$.

From eqns (1.8) and (1.9), with $\epsilon = 0$, we find the results corresponding to the important case of a *real* ϕ^2. For $\beta^2 < 4\zeta$

$$\alpha = -\beta/2, \quad \omega^2 = \zeta - \beta^2/4, \tag{1.14}$$

i.e. the stable motion of damped harmonic vibrations. For $\beta^2 \geq 4\zeta$

$$\alpha = -\beta/2 + \sqrt{(\beta^2/4 - \zeta)}, \quad \omega = 0, \tag{1.15}$$

i.e. static divergence for $\zeta < 0$ and static convergence for $\zeta > 0$.

2. THE EIGENVALUE PROBLEM

The separated differential equation of space corresponding to eqn (1.2) is

$$y''''(\xi) + \lambda y''(\xi) - \phi^2 y(\xi) \equiv 0, \quad \phi^2 = \zeta \pm i\epsilon, \tag{2.1}$$

and the boundary conditions according to Fig. 1 are

$$\begin{gathered} y(0) = y'(0) = y''(1) = 0, \\ y'''(1) + (1-\eta)\lambda y'(1) + (\mu\phi^2 - \kappa)y(1) = 0, \end{gathered} \tag{2.2}$$

with the non-dimensional follower, mass and spring parameters

$$\eta, \quad \mu = M/(\rho AL), \quad \kappa = KL^3/(EI). \tag{2.3}$$

Then the general solution to eqn (2.1) is

$$y(\xi) = C_1 \cosh(a\xi) + C_2 \sinh(a\xi) + C_3 \cos(b\xi) + C_4 \sin(b\xi), \tag{2.4}$$

and by inserting this in eqn (2.1) we find

$$\lambda = b^2 - a^2, \quad \phi = ab, \quad \begin{matrix} a \\ b \end{matrix} = \sqrt{\left[\mp\frac{\lambda}{2} + \sqrt{\left(\frac{\lambda^2}{4} + \phi^2\right)}\right]}. \tag{2.5}$$

Using the boundary conditions we obtain, for fixed parameters η, μ and κ the condition for a non-trivial solution as

$$D(\lambda, \phi) = D(a, b) = c_1 f_1 + c_2 f_2 + c_3 f_3 = 0 \tag{2.6}$$

where

$$c_1 = 2\phi^2 + (1-\eta)\lambda^2, \quad c_2 = (2\eta - 1)\lambda, \; c_3 = \mu\phi^2 - \kappa \tag{2.7}$$

and

$$\begin{aligned} f_1(\lambda, \phi) &= f_1(a, b) = 1 + \cosh(a)\cos(b), \\ f_2(\lambda, \phi) &= f_2(a, b) = b^2 - a^2 + ab \sinh(a)\sin(b), \\ f_3(\lambda, \phi) &= f_3(a, b) = \frac{b^2 + a^2}{ab}(b \sinh(a)\cos(b) - a\cosh(a)\sin(b)). \end{aligned} \tag{2.8}$$

Alternatively to this traditional form, the functions f_1, f_2, f_3, may be expressed as

$$\begin{aligned} f_1(\lambda, \phi) &= 1 + \frac{1}{2}(\cos(g) + \cos(\bar{g})), \\ f_2(\lambda, \phi) &= \lambda + i\frac{1}{2}(\cos(g) - \cos(\bar{g}))\phi, \\ f_3(\lambda, \phi) &= i(g \sin(\bar{g}) - \bar{g}\sin(g))h/\phi, \end{aligned} \tag{2.9}$$

where the complex quantities h, g, $\bar{g}$ are given by

$$\begin{aligned} &h = \frac{1}{2}(a^2 + b^2) \quad g = b + ia \quad \bar{g} = b - ia \\ &h^2 = \lambda^2/4 + \phi^2 \quad g^2 = \lambda + i2\phi \;\; \bar{g}^2 = \lambda - i2\phi. \end{aligned} \tag{2.10}$$

This latter form (2.9) is well suited for the differentiations to follow.

Possible static solutions, $\lambda_S \neq 0$ can be found from the simple case of eqn (2.6), where $\phi = 0$

$$[\eta + (1-\eta)\cos(\sqrt{(\lambda_S)})]\sqrt{(\lambda_S^3)} - \kappa[\sqrt{(\lambda_S)}\cos(\sqrt{(\lambda_S)}) - \sin(\sqrt{(\lambda_S)})] = 0, \tag{2.11}$$

and the natural frequencies ω_0 of the unloaded column follow from eqn (2.6) with $\lambda = 0$, i.e.

$$\begin{aligned} &\sqrt{(\omega_0^3)}[1 + \cosh(\sqrt{(\omega_0)})\cos(\sqrt{(\omega_0)})] \\ &\qquad + (\mu\omega_0^2 - \kappa)[\sinh(\sqrt{(\omega_0)})\cos(\sqrt{(\omega_0)}) - \cosh(\sqrt{(\omega_0)})\sin(\sqrt{(\omega_0)})] = 0. \end{aligned} \tag{2.12}$$

3. SOLUTION PROCEDURE AND RESULTS

The complex transcendental eqn (2.6) is solved with respect to the complex ϕ for given real load λ,

$$\phi = \phi(\lambda) \tag{3.1}$$

and this solution is easily obtained using the Newton–Raphson method. Thus we apply the rapidly converging iteration procedure

$$\phi_{n+1} = \phi_n + \Delta\phi_n, \quad \Delta\phi_n = -D(\lambda, \phi_n)\Big/\left(\frac{\partial D}{\partial \phi}\right)_{\lambda,\phi_n}. \tag{3.2}$$

Note that, due to the conjugate solutions to eqn (2.1) of the constant ϕ^2, we may limit ϕ to non-negative real as well as imaginary parts.

From eqns (2.6)–(2.10) we find $D_{,\phi} = \partial D/\partial\phi$

$$\begin{aligned} D_{,\phi} &= 4\phi f_1 + 2\mu\phi f_3 + c_1 f_{1,\phi} + c_2 f_{2,\phi} + c_3 f_{3,\phi} \\ f_{1,\phi} &= -i\frac{1}{2}(\sin(g)/g - \sin(\bar{g})/\bar{g}) \\ f_{2,\phi} &= i\frac{1}{2}(\cos(g) - \cos(\bar{g})) + \frac{1}{2}\phi(\sin(g)/g + \sin(\bar{g})/\bar{g}) \\ f_{3,\phi} &= i(g\sin(\bar{g}) - \bar{g}\sin(g))(h^{-1} - h\phi^{-2}) \\ &\quad - h\phi^{-1}\{g^{-1}(\sin(\bar{g}) - \bar{g}\cos(g)) + \bar{g}^{-1}(\sin(g) - g\cos(\bar{g}))\}. \end{aligned} \tag{3.3}$$

A small FORTRAN program with complex variables of less than 100 statements is able to solve a specific problem, $\phi = \phi(\lambda)$, for given η, μ, and κ within a CPU time of less than one second. Plotting with a standard precedure of interactive computer graphics produces the results presented in what follows.

Let us study the results of Fig. 2 in more detail. These results correspond to different *follower parameters* η, keeping $\mu = \kappa = 0$. The case of $\eta = 0.3$ shows stable motion (see eqn (1.14), (1.15)) for $\lambda < \lambda_S = 4.06$ ($\sqrt{(\lambda_S)} = \arccos(\eta/(\eta-1))$), and then unstable divergence for $\lambda > \lambda_S$ with increasing instability (α increases with λ). Now, for $\eta = 0.4$, the picture changes drastically. We still have stable motion for $\lambda < \lambda_{S1} = 5.29$, and then unstable divergence, but only within a definite domain $\lambda_{S1} < \lambda < \lambda_{S2} = 15.86$. The instability in this domain is bounded by $\alpha \le 3.3$. Stable motion is again the result in the domain $\lambda_{S2} < \lambda < \lambda_{F0} = 16.40$, and in the domain $\lambda_{F0} < \lambda < \lambda_{F\infty} = 17.9$, flutter instability may or may not occur, depending upon the actual damping β.

The function $\lambda_F = \lambda_F(\beta)$ is shown in the upper figure. For $\lambda > \lambda_{F\infty}$ flutter instability occur independent of damping. A sequence of stable-unstable domains as discussed here for $\eta = 0.4$ results for follower parameters in the interval $0.354 < \eta < 0.5$. For $\eta = 0.5$ the domain of unstable divergence degenerates to a point $\lambda_{S1} = \lambda_{S2} = \pi^2$. In the interval $0.5 < \eta < 1.0$ the results are stable motion for $\lambda < \lambda_{F0}$, then, in a domain $\lambda_{F0} < \lambda < \lambda_{F\infty}$, possible flutter instability depending upon damping, and for $\lambda > \lambda_{F\infty}$, flutter instability even when $\beta = \infty$. Finally, for $\eta > 1.0$, we get unstable divergence in tension, i.e. for $\lambda < \lambda_S = \text{arcosh}(\eta/(\eta-1))$; then, for $\lambda > \lambda_S$, the picture in general agrees with the above cases for $0.5 < \eta < 1.0$.

The next results in Fig. 3 correspond to different values for *mass parameter* μ, keeping $\eta = 1$, $\kappa = 0$. The general behaviour is stable motion for $\lambda < \lambda_{F0}$, then possible flutter instability for $\lambda_{F0} < \lambda < \lambda_{F\infty}$, and, definitively, flutter for $\lambda > \lambda_{F\infty}$. As seen from eqn (2.11), μ has no influence on static solutions λ, $\phi = \lambda_S, 0$, and additional mass therefore cannot force divergence to occur for $0.5 < \eta < 1.0$, but with increasing μ, the first natural frequency simply approaches zero. Note, that λ_{F0} decreases when adding end mass up to a given amount, but then increases again. This will be further discussed in Section 5. Note also in the upper figure that, for $\beta >$ about 10, $\lambda_F = \lambda_F(\eta)$ has changed, now being monotonically increasing.

Corresponding to different values of *spring parameter* κ, keeping $\eta = 1$, $\mu = 0$, we get the results of Fig. 4. Three different intervals of κ are to be considered. For $0 < \kappa < 34.8$, the general

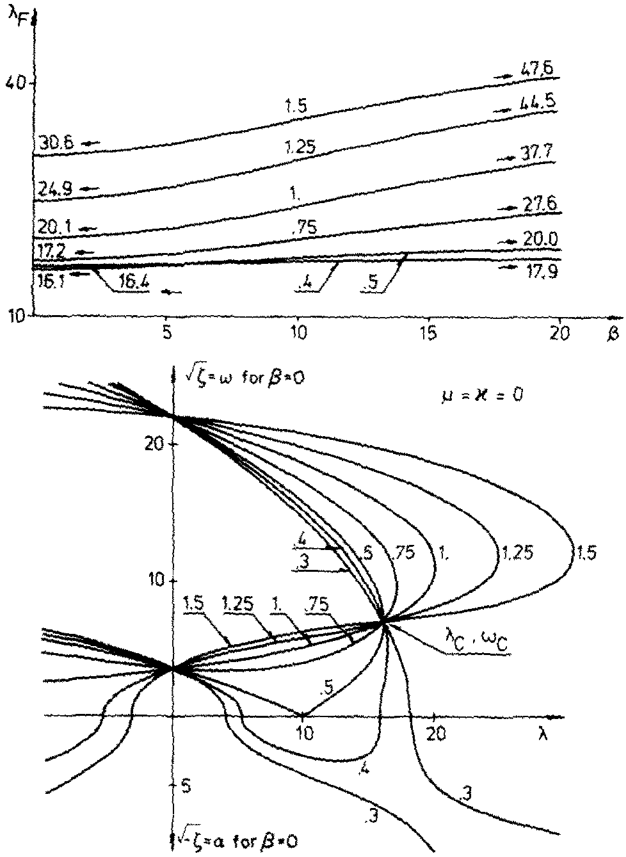

Fig. 2. For various values of the follower parameter η without end mass and end spring ($\mu = \kappa = 0$) the lower figure† shows the first two natural frequencies ω and the degree of instability α as a function of the force λ, assuming no damping (when $\beta \neq 0$ the results are given by eqns (1.14), (1.15)). The upper figure shows the onset of flutter λ_F as a function of the external damping β.

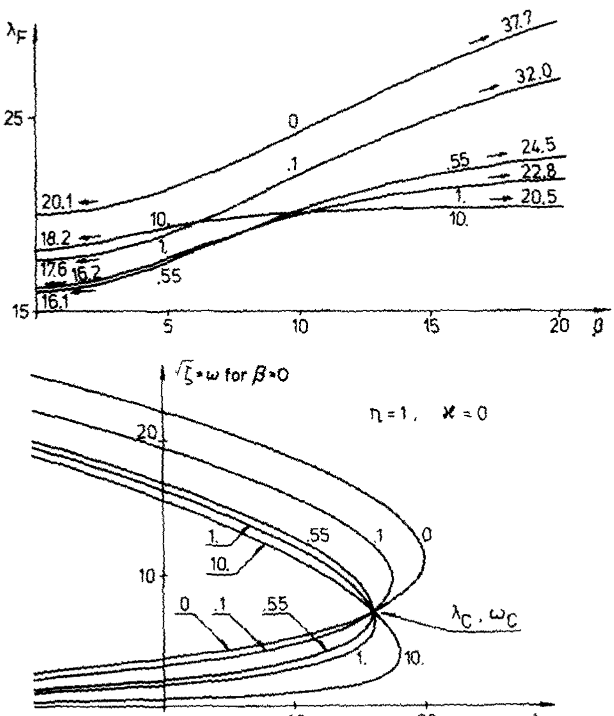

Fig. 3. For various values of concentrated end mass μ without end spring ($\kappa = 0$), and with a tangentially follower force ($\eta = 1$) the lower figure shows the first two natural frequencies ω as a function of the force λ, assuming no damping (when $\beta \neq 0$ the results are given by eqns (1.14), (1.15)). The upper figure shows the onset of flutter λ_F as a function of the external damping β.

†The results of the first quadrant may also be found in the early paper[6], recently pointed out in Ref. [4].

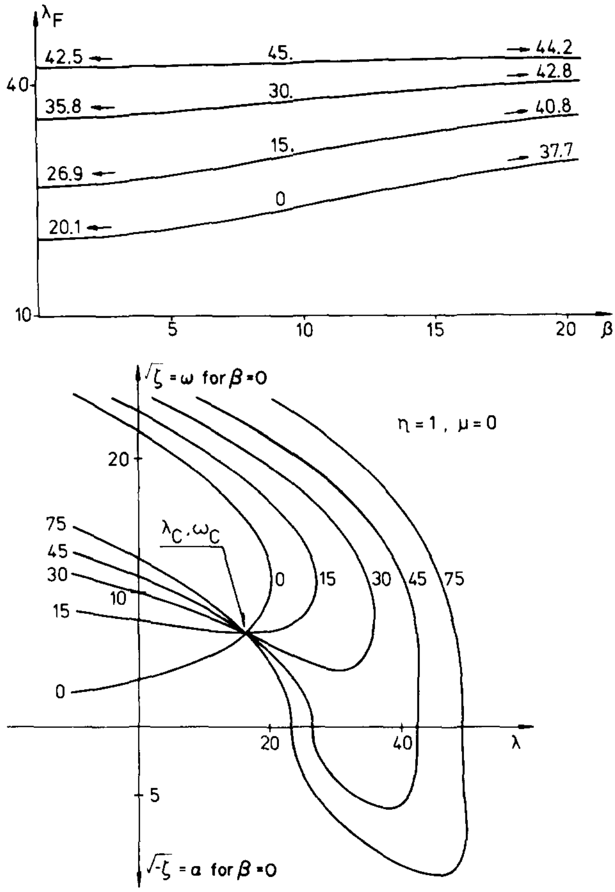

Fig. 4. For various values of the spring stiffness κ without end mass ($\mu = 0$), and with a tangentially follower force ($\eta = 1$) the lower figure† shows the first two natural frequencies ω and the degree of instability α as a function of the force λ, assuming no damping (when $\beta \neq 0$ the results are given by eqns (1.14), (1.15)). The upper figure shows the onset of flutter λ_F as a function of the external damping β.

picture is identical with $\kappa = 0$ in the sense, that the values of λ_{F0}, $\lambda_{F\infty}$ just increase with κ. For $34.8 < \kappa < \sim 50$ we have a domain of unstable divergence $\lambda_{S1} < \lambda < \lambda_{S2}$ before reaching λ_{F0}, and in the domain $\lambda_{S2} < \lambda < \lambda_{F0}$, stable motion result. Finally for $\kappa > \sim 50$, the only interesting point is λ_{S_1}, which separates stability from unstable divergence. The values of λ_S may be determined from eqn (2.11). We note for $\kappa = 75$, that unstable divergence may change to flutter with increasing load.

Taken as a whole, the results of Figs. 2–4 confirm and extend the results of the references. In addition, the curves clearly show the feature mentioned in the introduction. The common point, at which the natural frequency is *independent* of the concentrated mass, the support stiffness and of the follower angle of the force, is given by

$$\lambda_C, \omega_C = 16.05246, 7.05525. \tag{3.4}$$

The existence of such points for higher order pairs of eigenfrequencies is evident as well. In the section to follow we shall prove this fact.

4. INDEPENDENCE OF BOUNDARY CONDITIONS

From the first three boundary conditions (2.2) it follows that the eigenfunction is

$$y(x, \lambda, \phi) = y(x, a, b) = \cosh(ax) - \cos(bx) + [a \sin(bx) - b \sinh(ax)]f_4/f_5, \tag{4.1}$$

where

$$f_4(\lambda, \phi) = f_4(a, b) = a^2 \cosh(a) + b^2 \cos(b),$$

$$f_5(\lambda, \phi) = f_5(a, b) = ab[a \sinh(a) + b \sin(b)]. \tag{4.2}$$

†This result may also be found in a just published paper[14].

Note that the eigenfunction is explicitly independent of the parameters η, μ and κ. Note also that cases of $f_4 = f_5 = 0$ need further investigation.

Now, to prove the existence of λ_C, ω_C, we primarily define a_C, b_C by

$$\begin{gathered} a_C, b_C \text{ both real}, \quad \sin(b_C) \le 0 \\ a_C \cosh(a_C) = b_C, \quad b_C \cos(b_C) = -a_C. \end{gathered} \tag{4.3}$$

It then follows directly by inserting in eqns (2.8) and (4.2) that

$$f_1(a_C, b_C) = f_2(a_C, b_C) = f_3(a_C, b_C) = f_4(a_C, b_C) = f_5(a_C, b_C) = 0. \tag{4.4}$$

This means that the condition (2.6) is fulfilled independently of η, μ and κ. Further, it means that a more detailed analysis of the eigenfunction (4.1) is necessary. That there exists an infinite number of discrete points a_C, b_C that satisfy (4.3) is illustrated by the graphical display in Fig. 5.

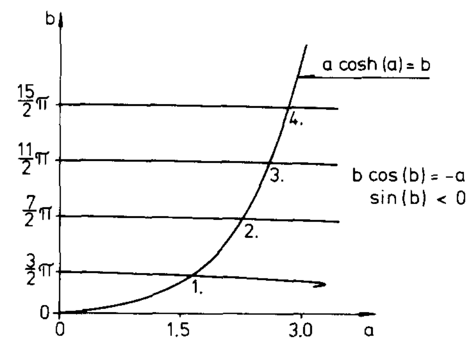

Fig. 5. Graphical solution of eqn (4.3).

Let us now concentrate on the eigenfunctions at the characteristic point. As $f_4(\lambda_C, \omega_C) = f_5(\lambda_C, \omega_C) = 0$ we have to perform a limit analysis in order to determine the eigenfunction (4.1). By the rule of l'Hospital we obtain

$$\left(\frac{f_4}{f_5}\right)_C = \left(\frac{\mathrm{d}f_4}{\mathrm{d}f_5}\right)_C = \left(\frac{\dfrac{\partial f_4}{\partial a} + \dfrac{\partial f_4}{\partial b}\dfrac{\mathrm{d}b}{\mathrm{d}a}}{\dfrac{\partial f_5}{\partial a} + \dfrac{\partial f_5}{\partial b}\dfrac{\mathrm{d}b}{\mathrm{d}a}}\right)_C, \tag{4.5}$$

the only unknown quantity being $\mathrm{d}b/\mathrm{d}a$. We shall determine this quantity for different path through λ_C, ω_C, specified by θ, where $\tan\theta = \mathrm{d}\omega/\mathrm{d}\lambda$. Using eqn (2.5) with $\omega = \phi$, we get

$$\tan\theta = \frac{(b\,\mathrm{d}a + a\,\mathrm{d}b)}{2(b\,\mathrm{d}b - a\,\mathrm{d}a)}, \tag{4.6}$$

which gives

$$\frac{\mathrm{d}b}{\mathrm{d}a} = \frac{2a\tan\theta + b}{2b\tan\theta - a}. \tag{4.7}$$

From eqns (4.5), (4.7) and (4.2) we can then determine $(f_4/f_5)_C$ as a function of θ, which is shown in Fig. 6.

This result shows that the eigenfunction (4.1) at the common characteristic point λ_C, ω_C can be any linear combination of $(\cosh(a_C x) - \cos(b_C x))$ and $(a_C \sin(b_C x) - (b_C \sinh(a_C x))$, which functions are plotted in Fig. 7 together with the cases of $(f_4/f_5)_C = -0.23$ and $= 0.5$ that correspond to $\theta = 0$ and $\pi/2$, respectively.

5. ONSET OF FLUTTER AND MINIMUM NATURAL FREQUENCY

In this section we want to study directly the influence of the boundary parameters η, μ and κ

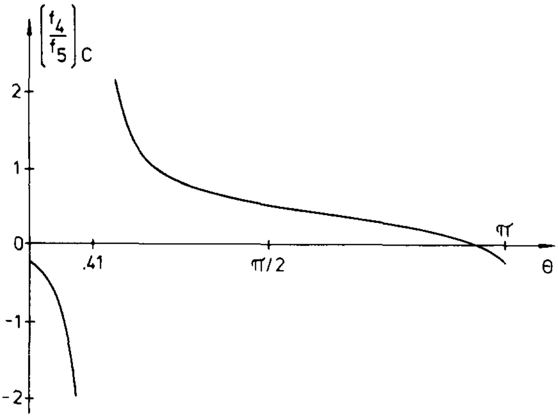

Fig. 6.

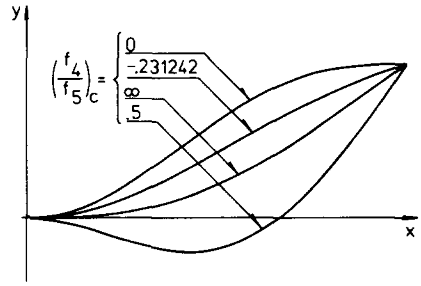

Fig. 7.

Fig. 6. Constant of the eigenmode at λ_C, ω_C as a function of the path ($\tan\theta = d\omega/d\lambda$).

Fig. 7. Normed eigenmodes at λ_C, ω_C corresponding to different characteristic curves through this point.

on the load λ_{F0} at which flutter occurs if we have no damping. However, we must remember that domains of instability may be actual for $\lambda < \lambda_{F0}$. Mathematically, the onset of flutter is characterized by

$$D(\lambda_{F0}, \phi_{F0}) = \frac{\partial D}{\partial \phi}(\lambda_{F0}, \phi_{F0}) = 0, \quad \phi_{F0}^2 \text{ real.} \tag{5.1}$$

Applying the Newton–Raphson method with λ as well as ϕ being the unknowns, we find the solutions to this problem, i.e.

$$\lambda_{n+1} = \lambda_n + \Delta\lambda_n, \quad \phi_{n+1} = \phi_n + \Delta\phi_n,$$
$$D(\lambda_n, \phi_n) + \left(\frac{\partial D}{\partial \lambda}\right)_{\lambda_n, \phi_n} \cdot \Delta\lambda_n + \left(\frac{\partial D}{\partial \phi}\right)_{\lambda_n, \phi_n} \cdot \Delta\phi_n = 0,$$
$$\frac{\partial D}{\partial \phi}(\lambda_n, \phi_n) + \left(\frac{\partial^2 D}{\partial \phi \partial \lambda}\right)_{\lambda_n, \phi_n} \cdot \Delta\lambda_n + \left(\frac{\partial^2 D}{\partial \phi^2}\right)_{\lambda_n, \phi_n} \cdot \Delta\phi_n = 0, \tag{5.2}$$

and thus directly find λ_{F0}, ϕ_{F0} as a function of the parameters η, μ and κ. In the formulation with the quantities g, $\bar{g}$ we see from eqns (2.7) and (2.9) that even the partial derivatives of the second order are not too complicated. As an example we find

$$f_{1,\phi\phi} = -\frac{1}{2}[g^{-2}(g^{-1}\sin(g) - \cos(g)) + \bar{g}^{-2}(\bar{g}^{-1}\sin(\bar{g}) + \cos(\bar{g}))]. \tag{5.3}$$

The results are shown in Figs. 8–10. For four cases of μ, κ the results λ_{F0}, $\omega_{F0}(\eta)$ are given in Fig. 8. Note that $(\lambda_{F0})_{\min} = \lambda_C$ independent of μ and κ, but appears at values η depending on μ, κ. Also the value η below which flutter does not exist depends on μ, κ.

Then, for four cases of η with $\kappa = 0$ the results λ_{F0}, $\omega_{F0}(\mu)$ are given in Fig. 9. Here we now find $(\lambda_{F0})_{\min} = \lambda_C$ independent of η but appearing at values μ depending on η. The curve corresponding to $\eta = 1.0$ comprises a modest refinement over results published earlier in [5] and [2]. Finally for four cases of η with $\mu = 0$, the results λ_{F0}, $\omega_{F0}(\kappa)$ are given in Fig. 10.

The minimum value of the first natural frequency $\omega_{\min}$ within a load range $\lambda_{\min} < \lambda < \lambda_{\max}$ is an important quantity that answers the question of latent instability ($\omega_{\min} = 0$ gives divergence). To locate $\omega_{\min}$ we must solve

$$D(\lambda, \phi) = \frac{\partial D}{\partial \lambda}(\lambda, \phi) = 0, \quad \phi^2 \text{ real,} \tag{5.4}$$

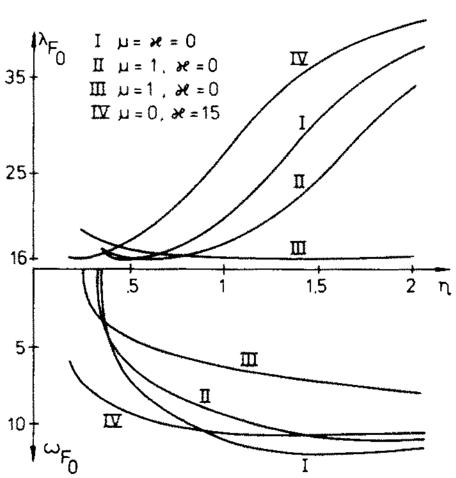

Fig. 8.

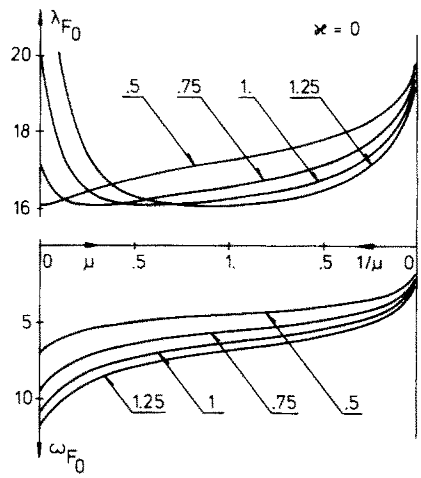

Fig. 9.

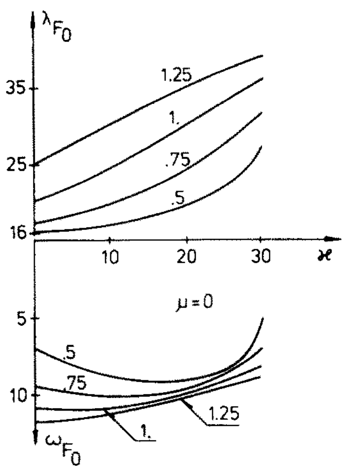

Fig. 10.

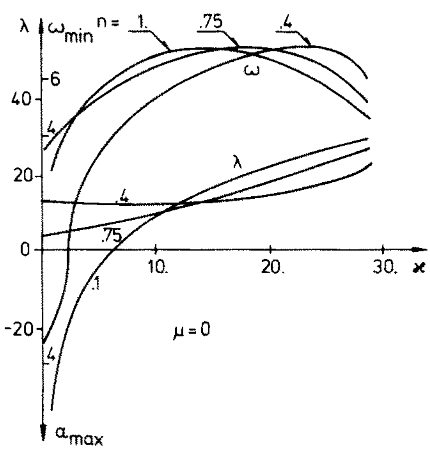

Fig. 11.

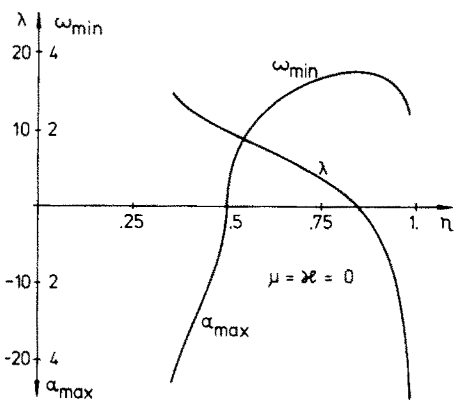

Fig. 12.

Fig. 8. The onset of flutter λ_{F0}, ω_{F0} with no damping ($\beta = 0$) as a function of the follower parameter η.

Fig. 9. The onset of flutter as a function of the end mass μ.

Fig. 10. The onset of flutter as a function of the end spring κ.

Fig. 11. The minimum natural frequency ω_{min} (resp. the maximum degree of instability α_{max}) as a function of the end spring κ together with the force λ at which these extremal values appear.

Fig. 12. The minimum natural frequency ω_{min} (resp. the maximum degree of instability α_{max}) as a function of the follower parameter η together with the force λ at which the extremal values appear.

which is done analogously to the procedure (5.2). Results are shown in Figs. 11 and 12.

Figure 11 shows that we have, in fact, solved optimum design problems defined as follows. Assume an active range of force $\lambda < \lambda_{F0}$, and design the support stiffness κ to maximize the minimum first natural frequency. Note that the "design" κ depends on η ($\mu = 0$), but the result $(\omega_{min})_{max} = \omega_C$ is independent of η. Parallel to this, Fig. 12 shows, for $\kappa = \mu = 0$, that $\omega_{min} = \omega(\lambda = 0)$ is obtainable with a specific follower angle of $\eta = 0.84$.

CONCLUSION

To answer the question of stability for a non-conservative problem, it is generally necessary to obtain the characteristic lines of instability in the load/frequency coordinate system. Furthermore, a good answer includes the sensitivities to changes in the variables of the problem such as boundary conditions. This means that parametric studies are necessary.

The study of the extended cantilever follower force problem with three boundary parameters does indeed give additional insight into the problem, besides proving the necessity of a dynamic formulation. First of all the existence of a force for which the natural frequency is independent of the boundary parameters is clearly demonstrated. This feature must be common to problems of similar kind.

The Newton–Raphson method is shown to be a very effective procedure for solving different statements of the problem without modelling to finite degree of freedom.

REFERENCES

1. H. Ziegler, *Principles of Structural Stability.* Blaisdell, Walton, Mass. (1968).
2. V. V. Bolotin, *Nonconservative Problems of the Theory of Elastic Stability.* Pergamon, Oxford (1963).
3. G. Herrmann, Stability of equilibrium of elastic systems subjected to nonconservative forces. *Appl. Mech. Rev.* **20**, 103–108, (1967).
4. H. Leipholz, *Six Lectures on Stability of Elastic Systems*, 2nd Edn. University of Waterloo, Canada (1974).
5. A. Pflüger, Zur Stabilität des Tangential Gedrückten Stabes. *Z. Angew. Math. Mech.* **85**, 191 (1955).
6. O. Petterson, *Ett Icke-Konservativt Knäckningsproblem, Festskrift til Professor Carl Forssell*, p. 96–104. Stockholm (1956).
7. H. König, Die Knickkraft beim Einseitig Eigespannten Stab unter Nichtrichtungstreuer Kraftwirkung, Der Stahlbau, **29**, 150–154 (1960).
8. Z. Kordas and M. Zyczkowski, On the loss of stability of a rod under a super-tangential force, *Arch. Mech. Sto.* **1**, 7–31 (1963).
9. G. Herrmann and R. W. Bungay, On the stability of elastic systems subjected to nonconservative forces, *J. Appl. Mech.* **31**(3), 435–440 (1964).
10. H. Leipholz, Über den Einfluss der Dämpfung bei nichtkonservativen Stabilitätsproblemen Elastischer Stäbe. *Ing. Arch.* **33**, 308 (1964).
11. S. Nemat-Nasser, S. N. Prasad and G. Herrmann, Destabilizing effect of velocity-dependent forces in nonconservative continuous systems. *AIAA J.* **4**, 1276–1280 (1966).
12. V. V. Bolotin and N. I. Zhinzher, Effects of damping on stability of elastic systems subjected to nonconservative forces. *J. Solids Structures* **5**, 965–989 (1969).
13. R. H. Plaut and E. F. Infante, The effect of external damping on the stability of Beck's column, *Int. J. Solids Structures* **6**, 491–496 (1970).
14. C. Sundararajan, Influence of an elastic end support on the vibration and stability of Beck's column. *Int. J. Mech. Sci.* **18**, 239–241 (1976).